

What drives spatial and temporal patterns within the residential range of two commercially important *Carcharhinus* species, and can residential patterns be used to predict broad scale displacements?

Katherine Bickerton

Submitted: August 2019



**A thesis submitted in partial fulfilment of the requirements for the degree of Master of
Research at Imperial College London**

Formatted in the journal style of the Marine Ecology Progress Series

Submitted for the MRes in Computational Methods in Ecology and Evolution

Declaration

I declare that the data used in this project was collected and provided by my co-supervisor Dr Matias Braccini, Western Australian Fisheries and Marine Laboratories, Government of Western Australia. I was provided with the raw dataset and carried out all processing, analysis and model development myself, with advice from Dr Matias Braccini and my primary supervisor, Dr David Jacoby, Institute of Zoology, Zoological Society of London. Dr Jacoby also provided training and an R code framework for network analysis, which I adapted for the dataset used.

1 Abstract

2 Large scale movements are common in shark species and are important for population connectivity
3 and ultimately species persistence. Due to overexploitation many shark species are at risk of
4 extinction including dusky sharks, *Carcharhinus obscurus*, and sandbar sharks, *Carcharhinus*
5 *plumbeus*. Both species are of commercial importance to fisheries in Western Australia however
6 little is known about their movements, especially within their home range. Network analyses, kernel
7 density estimates and residency indices were used to examine acoustic telemetry data detailing
8 residential movements of dusky and sandbar sharks within the Ningaloo Reef, WA. Dusky sharks,
9 which have been previously shown to migrate in WA, showed strong seasonal variation in network
10 density, residency patterns and depth use. A weaker seasonal variation occurred in sandbar sharks,
11 with higher residency and more consistent depth use than dusky sharks. Area of home range was
12 much lower in sandbar sharks and there was little variation between sexes of either species. The
13 greatest variation was found between individuals, indicating high behavioural plasticity in both
14 species. This complexity prevents the prediction of broad scale displacements from residential
15 movements. If broad migrations do occur in sandbar sharks in WA, they are likely to be occurring
16 either at greater depths than or on smaller scales than those of dusky sharks. A greater number of
17 acoustic receivers or use of bio-loggers would be recommended to increase accuracy of predictions,
18 and thereby aid fisheries management.

19 Introduction

20 The majority of sharks species are known to undertake large scale movements or regular migrations
21 (Speed et al., 2010, Espinoza et al., 2016), on the scale of tens to thousands of kilometres (Braccini
22 et al., 2016). These movements enable connectivity between populations, and can prevent genetic
23 drift and allow species persistence (Olds et al., 2012, Espinoza et al., 2016). However, broad scale
24 marine movements are difficult to track, especially in highly mobile species such as sharks, which
25 exhibit complex life histories (Baeyaert et al., 2018). This limits our understanding of the role that
26 sharks play within ecosystems, their habitat use and threats facing them (Espinoza et al., 2016).

27
28 A major threat to shark populations is overexploitation by commercial fisheries (Worm et al., 2013),
29 both as targeted catch and as bycatch. Estimates of shark take ranged from 6.4 - 7.9% of the global
30 population in 2013 (Worm et al., 2013), with high proportions of catches going unreported (Clarke
31 et al., 2006). Shark finning is widely acknowledged as a driver of shark mortality due to the high
32 value of fins in Eastern Asia (Clarke et al., 2013). Despite regulations against shark finning by
33 countries including Australia, Brazil, the USA and the European Union (Clarke et al., 2006,
34 Benavides et al., 2011, Braccini et al., 2017a), unregulated catches within Chinese waters and
35 illegal catches globally, lead to high error margins in estimates of decline (Worm et al., 2013).

36
37 Understanding movement is necessary for effective management and to mitigating against threats
38 such as shark finning (Espinoza et al., 2016). One method of monitoring movement is the use of
39 acoustic telemetry, which has traditionally be used over short spatial and temporal ranges (Braccini
40 et al., 2017c). Recent studies have adapted this method for long term monitoring of several coastal
41 shark species, allowing fine scale movements, (Lea et al., 2016), and broad scale displacements
42 (Espinoza et al., 2016) to be mapped. The use of network theory to analyse acoustic telemetry data
43 is also becoming common place in spatial studies (Jacoby and Freeman, 2016). Spatial network
44 analyses allow the interpretation of complex movement behaviours and can incorporate biotic and
45 abiotic factors (Lea et al., 2016). This enables effective conservation management of marine
46 species by building more accurate models of future movements (Jacoby and Freeman, 2016).

47
48 Movements of dusky, *Carcharhinus obscurus*, and sandbar sharks, *Carcharhinus plumbeus*, have
49 been monitored using acoustic telemetry (Braccini and Taylor, 2016) and fisheries catch logs along
50 the coast of Western Australia (Braccini, 2017). Both species are of commercial importance to WA
51 shark fisheries (Braccini, 2017) however both are also listed as Vulnerable by the IUCN Red List
52 (Musick et al., 2009a,b), therefore understanding their movements is important economically and
53 ecologically. As coastal species, they are at particularly high risk due to their close proximity to

humans, leading to easier exploitation (Espinoza et al., 2015) and a higher risk of habitat destruction (Speed et al., 2010). Additionally, both species have been previously overfished (Benavides et al., 2011, Braccini, 2017). Part of this take was for the Asian fin trade as sandbar sharks have a particularly high fin to body size ratio, increasing commercial value. (Braccini et al., 2017a).

Studies of *C. obscurus* and *C. plumbeus* have mainly examined juvenile movements and broad scale displacements. The two species are often grouped due to their similar life histories: both are relatively long lived, late to mature and have long gestation periods (Cortés, 2000, Benavides et al., 2011, Braccini et al., 2017a, Junge et al., 2019). These traits indicate that the persistence of mature individuals is key to population stability (Speed et al., 2010). There is evidence that mature *C. obscurus* undertake periodic large scale migrations (Hussey et al., 2009, Braccini et al., 2017b), however there is little evidence of this in mature *C. plumbeus* individuals (Mcauley et al., 2005). Furthermore, network analyses have not been applied to the movements of either species and individual behaviours have yet to be incorporated into movement models.

This study will examine the movements of mature dusky and sandbar sharks within their residential range, Ningaloo Reef, WA. Network analyses will be applied to long term acoustic monitoring data, and individual scale behaviours examined. The aims of the study are to (1) compare variation in acoustic network use within and between species, (2) compare variation in area and depth use between and within species and (3) compare residency patterns between and within species. All analyses will consider individual, sexual, seasonal and diel variation inside Ningaloo reef. This will then be linked to movement drivers within the species home ranges and whether residential movements can be extrapolated to give information regarding large scale movements, based upon known migrations of *C. obscurus* in WA.

78 **Methods & Materials**

79 **Data Collection**

80 In this study, acoustic telemetry was used to track the movements adult and sub-adult, as defined in
81 Braccini et al. 2017c, dusky sharks, *Carcharhinus obscurus*, and sandbar sharks, *Carcharhinus*
82 *plumbeus*, over an array of 437 acoustic receivers located along the coast of Western Australia
83 (Figure 1). Detection data was used from 2011 to 2018, with the first detection on the 2nd July 2011
84 and the last on the 5th September 2018. All shark tagging and deployment and retrieval of receivers
85 was carried out by the Government of Western Australia's Department of Fisheries (DoF), and the
86 raw dataset compiled by Dr Matias Braccini of the DoF.

87
88 A total of 207 adult or sub-adult sharks, 103 *C. obscurus* and 104 *C. plumbeus* were implanted with
89 acoustic tags. All tagging occurred annually in the austral autumn and winter, between 2011 and
90 2017 (with the exception of 2016), by experienced taggers during surveys by the DoF. All sharks
91 tagged were measured and sexed, and date and location of release recorded. Tagging was carried
92 out along the coast between Broome and Esperance, WA, mainly within the Ningaloo reef (Figure
93 2). For more details on the tagging procedure please refer to Braccini et al. 2017a.

94
95 The receivers were split into northern (Figure 1a) and southern arrays (Figure 1b & c). In the north,
96 57 receivers were deployed in three line arrays between the Tantabiddi Creek and Coral Bay,
97 21.5°S - 23.5°S, 113.5°E - 114°E, with a depth range of 2-161 meters. Although shark tagging
98 occurred further to the north, cyclone exposure and the width of the continental shelf prevented
99 more receivers from being deployed. The 380 southern receivers were split into five line arrays, two
100 on the west coast and three on the south coast between Perth and the Recherche Archipelago,
101 31.0°S - 35.5°S, 114°E - 124°E, with a depth range of 9-198 meters. The receivers were initially set
102 up to mitigate against white and tiger shark attacks in the south (McAuley et al., 2016), and to
103 monitor coral reef fish spawning in the north (Babcock et al., 2017), therefore are in line arrays as
104 opposed to the grids that are used in most network analysis experiments. For full details of the
105 receivers used and data recovery, see Braccini et al. 2017a,b.

106
107 During the 8 years of monitoring, 130 of the 207 sharks tagged were detected, 68 *C. obscurus* and
108 62 *C. plumbeus*, across 183 of the 437 receivers (Table 1). The majority of detections (97.4%, total
109 = 196507) occurred within the residential range of both populations, the Ningaloo reef. Within the
110 Ningaloo reef, 118 sharks were detected across 57 receivers on more than five separate days. For
111 each detection, the location, time, date, depth and tag code were recorded. This dataset, the
112 demographic data from tagging, and the location and depth of each receiver, were used in analysis.

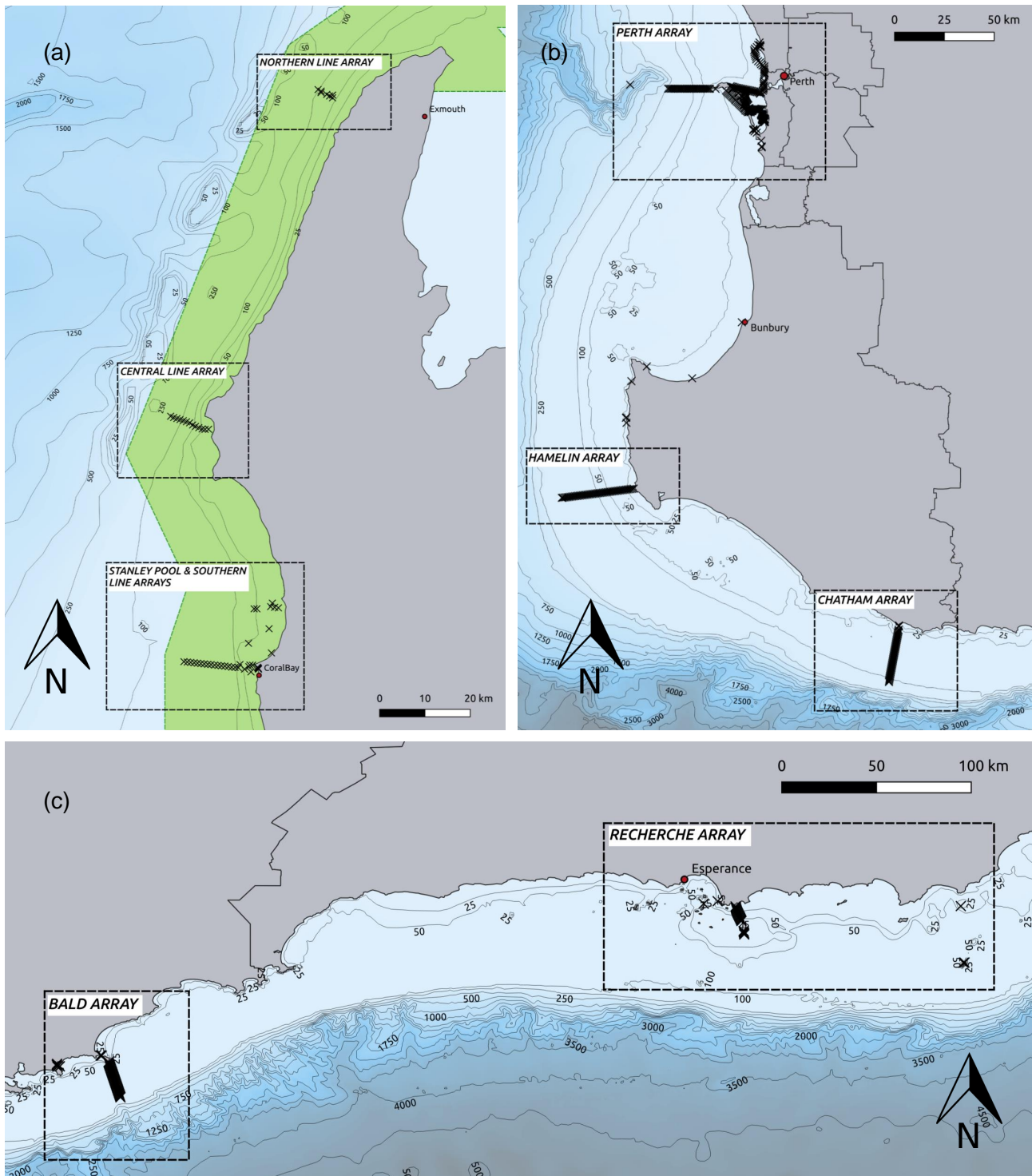


Figure 1: Distribution of acoustic receivers in Western Australia, each cross (x) representing an individual receiver. (a) Northern receivers within the Ningaloo reef, total = 57, Northern Line array = 7, Central Line array = 13 and Stanley Pool and Southern Line arrays = 37. Green shading represents the Ningaloo marine World Heritage Site (Flanders Marine Institute, 2013). (b) Perth and South Western receivers, total = 324, Perth array = 232, Hamelin array = 48 and Chatham array = 44. (c) Southern receivers, total = 56, Bald array = 33 and Recherche array = 23. This map was generated using QGIS (QGIS Development Team, 2019), with a base map shapefile (Australian Bureau of Statistics, 2011), bathymetric contour shapefile (GEBCO Compilation Group, 2019) and bathymetry raster (Whiteway, 2009).

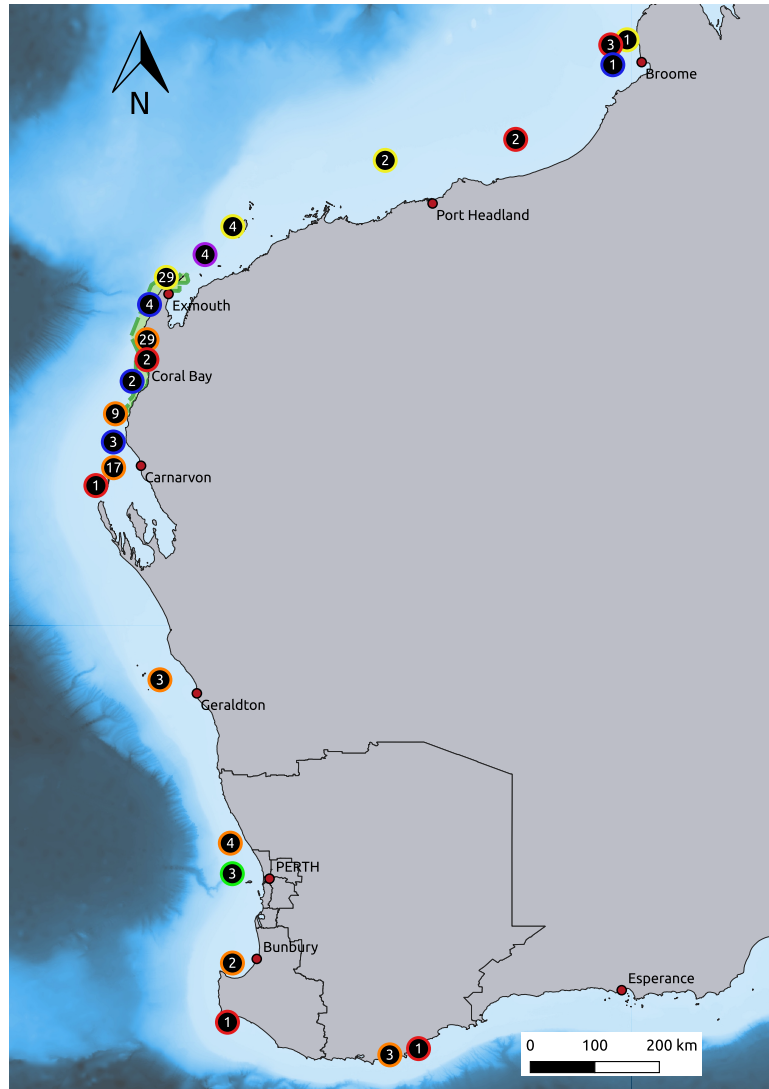


Figure 2: Locations of shark tagging of sharks detected between 2011 and 2018 ($n = 130$). The number within each circle gives the number of sharks tagged at that location and the coloured border gives the year of tagging (yellow = 2011, orange = 2012, red = 2013, purple = 2014, blue = 2015, green = 2017, no tagging occurred in 2016 & 2018.) This map was generated using QGIS (QGIS Development Team, 2019), with a base map shapefile (Australian Bureau of Statistics, 2011) and bathymetry raster (Whiteway, 2009).

Table 1: Summary of detected shark demographics, where M, F and U stand for male, female and unknown respectively. Size range represents fork length, measured at time of tagging in meters. Time monitored is the number of days between tagging and the most recent detection.

Species	Sex				Size Range (m)	Time Monitored (days)
	M	F	U	Total		
<i>Carcharhinus obscurus</i>	24	43	1	68	1.5 - 2.98	7 - 1987
<i>Carcharhinus plumbeus</i>	19	43	-	62	1.22 - 1.58	8 - 1976
Total	43	86	1	130	-	-

Data Analysis

All data manipulation, analysis and model building was carried out using R version 3.6.1 (R Core Team, 2015). The tidyverse package (Wickham, 2017) was used for all data manipulation and plots and the lubridate package (Grolemund and Wickham, 2011) for formatting temporal data. Analyses used detections from the Ningaloo reef arrays exclusively (defined as any detection north of 24°S), as the majority detections of both species occurred within the reef (Braccini et al., 2017c). The analysis was split into four sections: spatial network analysis, home range estimation using centres of activity, residency patterns using a residency index, and detection patterns examining detections per day. A combination of analyses methods were used as although spatial networks can be used to explain movement dynamics, more traditional approaches can also provide valuable insight (Baeyaert et al., 2018).

In each section of the analyses, linear mixed models were used to examine the relationship between the response variable (network density, kernel utilisation distribution, residency index and depth index respectively) and a range of fixed explanatory variables, using the lme4 R package (Bates et al., 2015). Linear mixed models were chosen so non-independent individual variation could be included as a random variable, and as data was linear but not normally distributed in all cases. Between and within species variation were both modelled. Model distribution was chosen by comparing the fit of quantile-quantile plots against normal, log normal, Poisson, negative binomial and gamma probability distributions, using the car (Fox and Weisberg, 2019) and MASS (Venables and Ripley, 2002) packages in R. Test files were then generated, and each model tested, then outputs compared against the original data to check model fit, using the merTools package (Knowles and Frederick, 2019).

Fixed explanatory variables used were species, sex, season, time of day and migratory status. For

sex, one individual of unknown sex was excluded. Season was assigned based upon Austral seasons (Summer: December-February, Autumn: March-May, Winter: June-August, Spring: September-November). Time of day, either day or night, was defined average sunrise and sunset times per month across the years of monitoring (Geoscience Australia, 2015). Data was not stratified by year due to small sample sizes in several years. In models examining *C. obscurus*, migratory status was used as an explanatory variable as the species are known to be resident in Ningaloo but make periodic migrations south (Braccini et al., 2017b). Migratory individuals were those that made at least one return journey between the Ningaloo receiver arrays and the southern arrays and were detected on least five days. Five *C. obscurus* were only detected in the southern arrays and are shown to be younger individuals, most likely moving north from their nursery grounds, by Braccini et al. 2017b, so were also excluded from this study. Model selection was carried out using the Akaike Information Criterion (AIC), for each subset with best fit denoted by the lowest AIC value and highest marginal R^2 value, calculating using the MuMIn package for R (Barton, 2019), defined as individual variance explained (Nakagawa and Schielzeth, 2013). Each model was then checked using a traditional likelihood ratio test (ANOVA) comparing each model with a null model.

Spatial Networks

Network analysis examines the relationship between nodes and the connections between them, known as edges (West, 2001). In this system, the receivers are used as the nodes and individual shark movements as edges. Spatial networks were built for each species, sex and individual, then individual networks were subset by time of day and season. To generate each network, movements between receivers were calculated. The R package igraph (Csardi and Nepusz, 2006) was used to calculate adjacency matrices and edge lists for each movement between receivers. Network density was calculated and is the number of edges in each network divided by the total number of possible edges (Mourier et al., 2018), representing the proportion of the total residential area (within the Ningaloo arrays) used by each individual. Network visualisations were generated using the rgdal package for R (Bivand et al., 2019) to aid analysis.

Network density was used as the response variable in each linear mixed model with a log normal probability distribution, and species, sex, season, time of day and migratory status (*C. obscurus* only) as fixed explanatory variables. Any individuals <5 movements detected were excluded.

170 Home Range

171 To investigate home range, centres of activity were calculated for each individual, and subset for
172 each season and time of day. The centre of activity (COA) of each shark was calculated using the
173 VTrack package (Campbell et al., 2012), which calculates a weighted mean position based upon
174 detection locations. This method was evaluated and found to be reasonably accurate within an array
175 when compared to actively tracked individuals (Simpfendorfer et al., 2002). The COAs were used to
176 calculate minimum convex polygons (MCPs), which define the minimum area containing all
177 detections of an individual, centred on the COA. To calculate these, a minimum of four detections at
178 different receivers within the Ningaloo arrays were required, individuals that did not meet this
179 criterion were excluded. MCPs give an estimate of the extent of range within the Ningaloo reef
180 however a better estimate for home range is a kernel utilisation distribution (KUD). This method uses
181 location and density of detections in a probability density function to estimate the probability of the
182 individual being found within a certain area (Jacoby and Freeman, 2016). Core or home range was
183 then calculated as the area within the KUD where the most activity occurred, with a size of 50% of
184 the total KUD. MCPs and KUDs were calculated using the adehabitatHR package (Calenge, 2006),
185 packages sp (Pebesma and Bivand, 2005, Bivand et al., 2013) and rgdal (Bivand et al., 2019) were
186 used to transform between coordinate systems and export shapefiles of KUD areas respectively.

187
188 KUD area was used as the response variable for linear mixed models examining home range. The
189 models used a gamma distribution, and species, sex, season, time of day and migratory status (*C.*
190 *obscurus* only) as fixed explanatory variables. Individuals with <5 movements in a subset were
191 excluded, consistent with the overall COA calculations.

193 Residency Patterns

194 To study residency patterns within Ningaloo reef, a residency index was calculated for each
195 individual over the monitoring period, and subsets taken and calculated for season, time of day and
196 season stratified by time of day. The residency index was defined as the number of days detected
197 within the Ningaloo arrays as a proportion of the number of days monitored, between release and
198 last detection (Espinoza et al., 2016). Values near 1 indicate a high residency to the reef and 0 a low
199 residency.

200
201 Residency index was used as the response variable in the linear mixed models, with a log probability
202 distribution (as the data was proportional). Fixed explanatory variables used were species, sex,
203 season, time of day and migratory status (*C. obscurus* only). Individuals detected on <5 unique

204 days were excluded as sample size was too small to give an accurate measure of residency.

205

206 **Detection Patterns**

207 Number of detections per day per individual were calculated then split by depth to allow investigation
208 of depth use. Depth of detections were split into 25m bands, with receiver depths ranging between 1
209 161 meters within Ningaloo reef.

210

211 Mixed models were built using number of detections per day as response variable, with a log normal
212 distribution. Fixed explanatory variables used were sex, species, depth band, time of day, season
213 and migratory status (*C. obscurus* only). To further examine depth patterns, fixed variables were
214 tested as random variables with depth band as the only fixed variable, within further mixed models,
215 again using a log normal distribution. Individuals with <5 unique days detected and depth bands
216 with fewer than 5 detections were excluded in consistency with the rest of the study.

217 Results

218 To examine movement behaviour of dusky, *Carcharhinus obscurus*, and sandbar sharks,
219 *Carcharhinus plumbeus*, generalised linear mixed effect models (GLMMs) were used with spatial
220 network density, kernel utilisation distribution area (KUD), residency index (RI) and detections per
221 day as response variables. Within and between species variation was accounted for by modelling
222 both species together and separately. Individual shark ID was used as a random effect to account
223 for individual variation and non-independence of related individuals and all models used a single
224 fixed explanatory variable. The best model for each response variable was selected using the
225 Akaike Information Criterion (AIC), where the lowest value indicates best fit (Bolker et al., 2009) and
226 variance explained (R^2), where possible (Nakagawa and Schielzeth, 2013). Traditional null model
227 comparisons using likelihood ratio tests were also used as a third test of model fit however outputs
228 from these were interpreted with caution as p-values are considered less relevant when using mixed
229 effect models (Posada and Buckley, 2004). Models with multiple explanatory variables were tested
230 and found, in all cases, to explain less of the variance and have a higher AIC value than models with
231 single variables. Full model outputs can be found in the Appendices.

232 Spatial Networks

233 Network density was used as the response variable for all spatial network models and gives the
234 proportion of edges in the network used out of all possible edges (Mourier et al., 2018). Individual
235 variation accounted for between 65.5 - 91.2% of deviance explained in each model, indicating high
236 intra-species variation in network use. Detailed outputs of all models in this section are given in
237 Appendix Table A1.

238
239 Species, as a fixed effect, had a relatively low AIC value (65.60) and accounted for 4.7% of
240 deviance, with sandbar sharks using a higher proportion of the network than dusky sharks, on
241 average (Figure 3). Sex had the highest AIC (67.52) and explained 4.9% of deviance across both
242 species, with males using a slightly higher proportion of the network overall but not significantly so.
243 Season gave the lowest value of AIC (65.09) and accounted for 3.2% of deviance. Highest network
244 density occurred in Summer then decreased through Autumn into Winter, then increased again in
245 Spring (Figure 3). Network density did not vary significantly with time of day, accounting for only 1%
246 of deviance.

247
248 When subset for *C. obscurus*, sex accounted for 13% of deviance, with males having a higher
249 network density than females. Seasonal variation gave the lowest AIC value (48.39) and accounted
250 for 15.9% of deviance, with the same pattern as before, highest in summer, decreasing through

251 autumn to winter then increasing again in spring (Figure 3). Time of day and migratory status
 252 accounted for 2.1% and 3.4% of deviance respectively and showed very little variation.
 253
 254 Network density in *C. plumbeus* again showed greatest variation and lowest AIC value (5.12)
 255 seasonally, which accounted for 3.3% of deviance. The highest value of network density occurred in
 256 summer and decreased through to winter as before, however continued to decrease in spring
 257 (Figure 3). Time of day and sex showed minimal variance and gave significantly higher AIC values
 258 of 8.46 and 9.42 respectively.

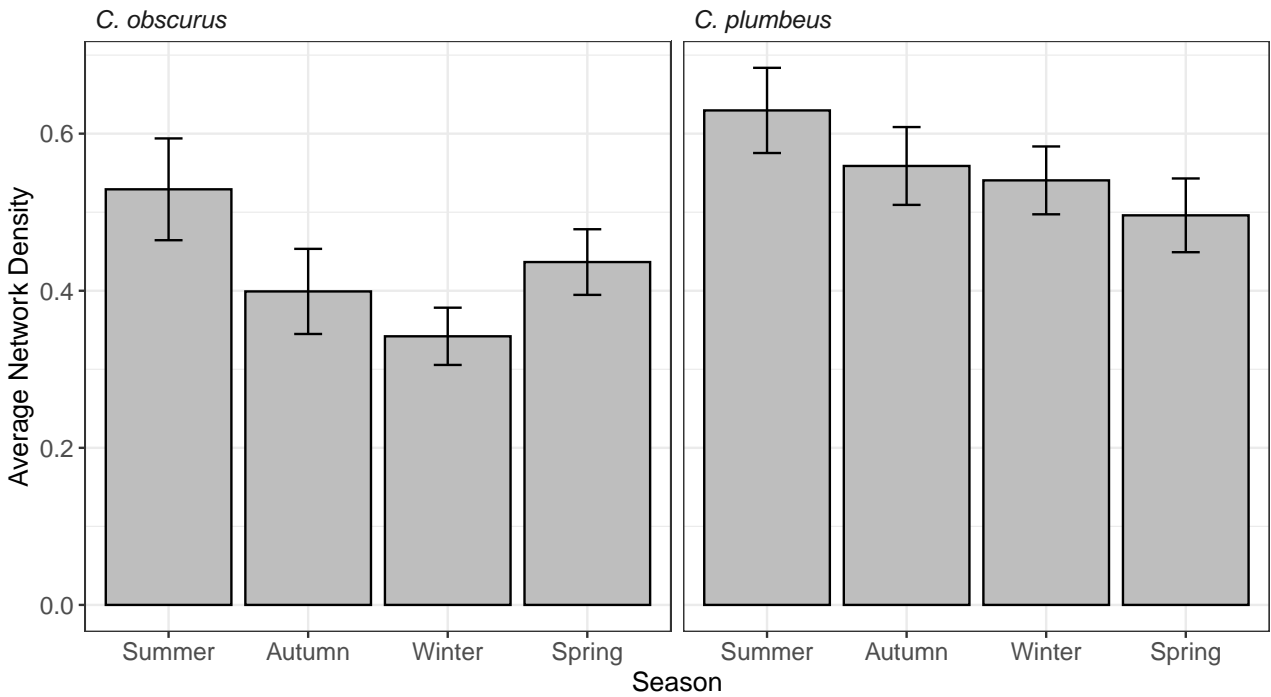


Figure 3: Seasonal variation in network density of *Carcharhinus obscurus* (n = 53) and *Carcharhinus plumbeus* (n = 58). Bars give mean average network density and error bars give standard error. Seasons are defined as standard Austral seasons.

259 Home Range

260 Kernel utilisation area (KUD) was used as the response variable in each home range model, and
 261 gives the size of the core range of each individual, based upon detection number and location
 262 (Jacoby and Freeman, 2016). Model were selected using AIC and with reference to likelihood ratio
 263 tests as R^2 lack accuracy for gamma distributed models. Individual variation had a significant effect
 264 in all models when tested against a null linear model.
 265

266 The largest variation in KUD was between species, with the lowest AIC values for both season and
 267 time of day subsets (334.9 and 285.8), and a significant difference with the null GLMM (ANOVA: χ^2_4

268 = 12.13, $p < 0.001$). *C. obscurus* had a larger average kernel area than *C. plumbeus*. Intraspecies
 269 variation in area was also much lower in *C. plumbeus* than in *C. obscurus*. KUD showed little
 270 variation with sex, season, time of day or migratory status in all subsets. All model outputs are given
 271 in Appendix Table A2.

272 Residency Patterns

273 Residency index (RI) was calculated as days detected within the Northern receiver arrays (Figure
 274 1a), as a proportion of days monitored, and used as the response variable for all residency models.
 275 Individual variation was significant in all models, accounting for between 77.6 - 99.5% of deviance
 276 explained by each model. Full model outputs are available in Appendix Table A3.

277

278 There was little variation in RI with species and sex, and relatively high values of AIC
 279 (-345.8,-644.9), and low deviance explained (3.8% and 1.8%). RI varied with season, with the
 280 lowest AIC value of -710.7. RI decreased in summer and spring but was more consistent in autumn
 281 and winter, however this only explained 3.7% of the deviance. Seasonally, average sandbar RI was
 282 higher than dusky (Figure 4). Time of day also led to variance in RI, with residency being slightly
 283 higher at night, however only 0.6% deviance was explained by this model.

284

285

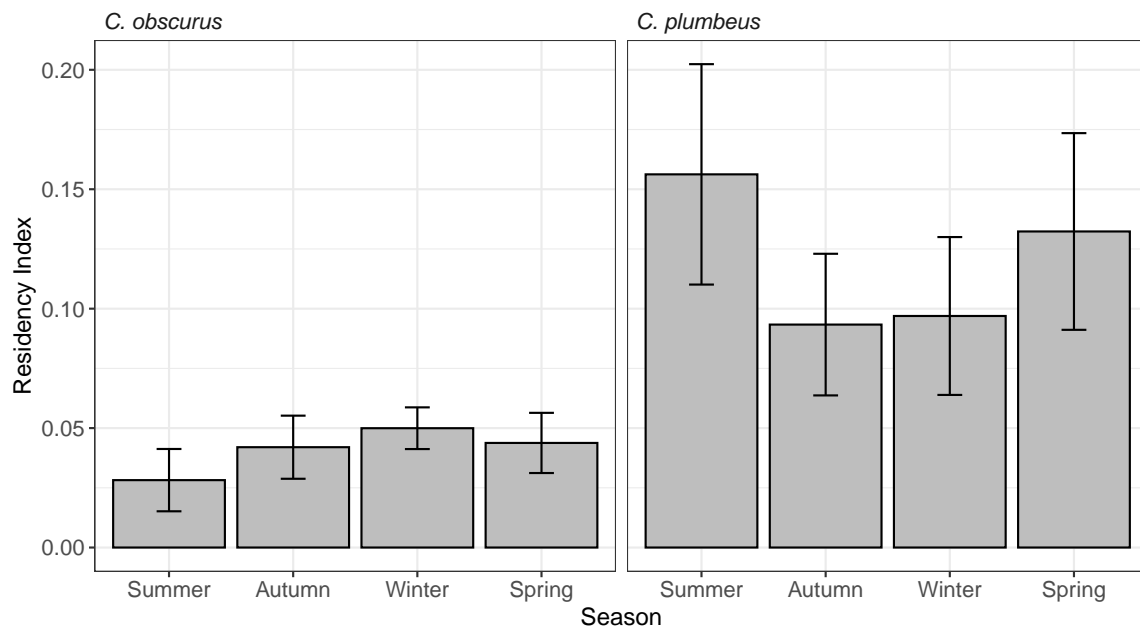


Figure 4: Seasonal variation in residency index of *Carcharhinus obscurus* (n = 51) and *Carcharhinus plumbeus* (n = 59). Bars give mean average residency index and error bars give standard error. Seasons are defined as standard Austral seasons.

286 RI varied more significantly by season within the *C. obscurus* subset, explaining 22.2% of deviance,
287 and having the lowest AIC of -461.8. RI was lowest in the summer, then increased through autumn
288 and winter, then decreased again in spring (Figure 4). Time of day also had a low value of AIC
289 within it's subset (-740.5), with a slight increase in RI at night but only this accounted for 5% of
290 deviance. Sex explained 18.2% of deviance in RI, with higher RI in females, but a high AIC value. RI
291 did not vary with migratory status.

292

293 Seasonal variation was also present in the *C. plumbeus* subset, with a AIC of -349, with values
294 highest in summer, decreasing until Spring but only by a small proportion (Figure 4). Time of day
295 and sex had very little effect on RI for sandbars, with a slightly higher average RI at night and in
296 males.

297 **Detection Patterns**

298 Number of detections per day was used to examine detection patterns and calculated for each
299 individual, per depth band (set at 25m intervals). AIC were all exceptionally high and R^2 values very
300 low for all models examined in comparison to all other response variables. Individual variation
301 accounted for between 12.0 - 24.3% of deviance in each model and all fixed effects accounted for
302 <0.1%. See Appendix Table A4 for all model outputs.

303

304 Depth of detections, although have a low R^2 and high AIC value, did highlight seasonal trends.
305 Detections of *C. obscurus* between 0-25m and over 100m only occurred in winter and spring,
306 whereas detections between 25-100m occurred in all seasons. None were detected above 125m.
307 Detections of *C. plumbeus* between 0-125m occurred during all seasons, however the number of
308 detections at depths below 25m were significantly lower. *C. plumbeus* were detected at depths
309 >125m but only during winter and autumn. The northern lines array in Figure 5 shows the near
310 constant distribution of sandbar sharks (orange) throughout the year and absence of dusky sharks
311 (purple) in the summer. The central line array, Figure 6, shows the decrease in dusky sharks in
312 summer and a more restricted depth range in the spring. The Stanley Pool and southern line arrays,
313 Figure 7, show a decrease in dusky sharks through spring and summer, as well as more shallow
314 water detections than in sandbars. Figures 5-7 all highlight the greater depths at which sandbars are
315 found throughout the year.

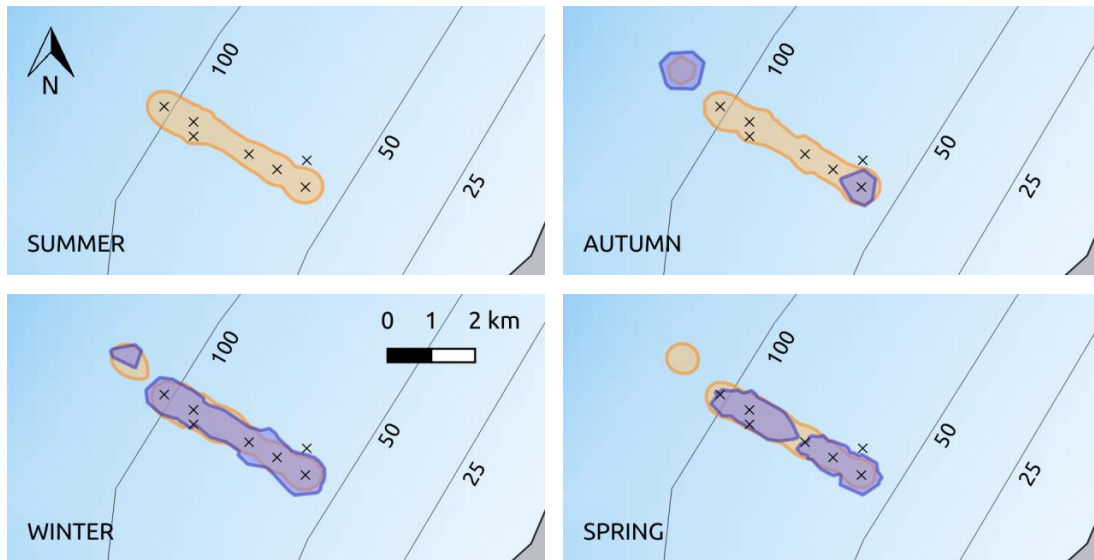


Figure 5: Seasonal variation in core kernel utilisation areas of *Carcharhinus obscurus* (purple) and *Carcharhinus plumbeus* (orange), within the northern line array, Ningaloo reef, WA. Black crosses (x) show acoustic receiver locations and water depth is given parallel to each bathymetry contour. This map was generated using QGIS (QGIS Development Team, 2019), with a base map shapefile (Australian Bureau of Statistics, 2011), bathymetric contour shapefile (GEBCO Compilation Group, 2019) and bathymetry raster (Whiteway, 2009).

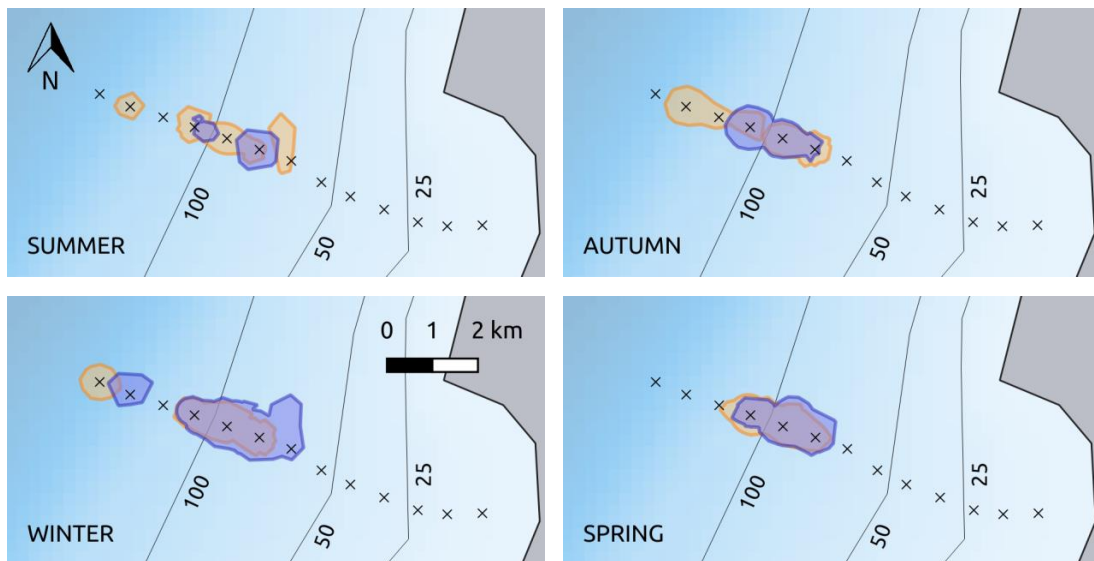


Figure 6: Seasonal variation in core kernel utilisation areas of *Carcharhinus obscurus* (purple) and *Carcharhinus plumbeus* (orange), within the central line array, Ningaloo reef, WA. Black crosses (x) show acoustic receiver locations and water depth is given parallel to each bathymetry contour. This map was generated using QGIS (QGIS Development Team, 2019), with a base map shapefile (Australian Bureau of Statistics, 2011), bathymetric contour shapefile (GEBCO Compilation Group, 2019) and bathymetry raster (Whiteway, 2009).

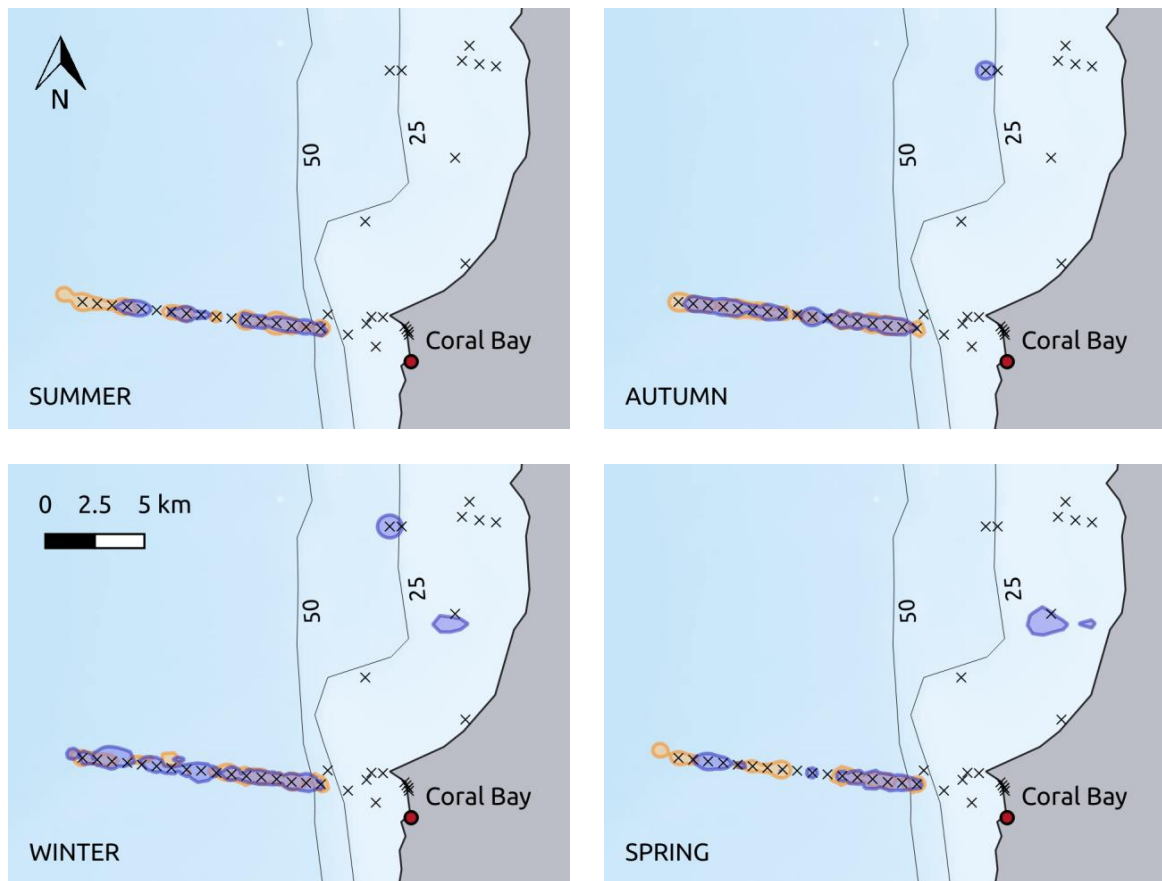


Figure 7: Seasonal variation in core kernel utilisation areas of *Carcharhinus obscurus* (purple) and *Carcharhinus plumbeus* (orange), within the Stanley Pool and southern line arrays, Ningaloo reef, WA. Black crosses (x) show acoustic receiver locations and water depth is given parallel to each bathymetry contour. This map was generated using QGIS (QGIS Development Team, 2019), with a base map shapefile (Australian Bureau of Statistics, 2011), bathymetric contour shapefile (GEBCO Compilation Group, 2019) and bathymetry raster (Whiteway, 2009).

316 Discussion

317 This study aimed to address the drivers of residential movements and whether they could be used to
318 predict large scale movements by comparing variation in acoustic network use, area and depth use
319 and residency between and within species. This was examined using acoustic telemetry data on two
320 species of shark dusky, *Carcharhinus obscurus*, and sandbar, *Carcharhinus plumbeus*.

321 Network Use

322 Spatial network analysis was used to assess use of the reef. Network density was chosen as the
323 best network metric for this system as it contained line arrays as opposed to conventional grid
324 arrays, and spanned a much larger area, rendering any network metric reliant on equal spacing of
325 nodes meaningless. Network density is not as dependent on this, as it gives a proportion of the
326 edges used out of the total possible edges, as opposed to the length of each edge.

327
328 Network density showed very little variance between species, indicating both species use similar
329 proportions of the reef. When split by season, dusky sharks showed a distinct pattern, with
330 proportion of edges used decreasing significantly in winter then increasing again in the summer.
331 This could be linked to migratory individuals moving south for summer migration and thereby using a
332 higher proportion of receivers, then only using a relatively small proportion when resident during the
333 winter. The seasonal pattern in sandbar sharks was not as distinct, with the highest in summer and
334 a steady decrease through to spring, but only a small overall change. This indicates less change in
335 reef use and therefore potentially a lower likelihood of migration. Many species of shark, such as
336 lemon, leopard, whitetip reef and grey reef sharks, show increased movement and therefore higher
337 network density at night (Speed et al., 2010), however no evidence of this was detected in either of
338 the study species, which had a fairly consistent daily network density.

339
340 Sex accounted for 13% of deviance in network density of *C. obscurus*. This has been observed in
341 grey reef sharks, *C. amblyrhynchos*, in eastern Australia (Espinoza et al., 2015), but was linked with
342 larger size of males leading to a larger number of movements. Size shows very little variation with
343 sex in dusky sharks (Braccini et al., 2017b), however the majority of males tagged were migratory so
344 the difference between sexes is more likely to be correlated with proportions migrating than size.
345 This could not be shown statistically in this study due to a very low sample size of non-migratory
346 dusksies. The lack of difference in network density with sex in *C. plumbeus* is more similar to that of
347 bull *C. leucas* and silvertip sharks *C. albimarginatus* no differentiation in network density with sex
348 (Espinoza et al., 2015).

349

350 Variation in network density did not correlate with migratory status in *C. obscurus* suggesting use of
351 the reef is more linked closely individual variation, rather than population dynamics, as seen in Lea
352 et al. 2016.

353 **Area & Depth Use**

354 KUD area showed no variance with sex, season or time of day in either species, showing annual
355 consistency with the area used. Increase in home range has previously been found in male grey
356 reef sharks however size often correlates with home range and male grey reef sharks are larger
357 than females (Speed et al., 2010), explaining the variation, whereas this size difference is not
358 present in dusky or sandbar sharks. Dusky sharks had significantly larger home ranges than
359 sandbars, with a difference of 1km between average core ranges. This could be due to greater
360 variation in movement of the migratory dusky sharks, or more movements of dusky sharks due to
361 larger size (Braccini et al., 2017b), which is correlated with larger range (Speed et al., 2010)

362
363 Use of depth also varied between sandbar and dusky sharks. In Figure 6&7, sandbars are regularly
364 detected at the higher receiver depths whereas the depth range of dusky is much more restricted.
365 Additionally, in Figure 7, dusky sharks are the only species regularly occur in depths of less than
366 25m. Dusky sharks could also be taking advantage of upwelling that often occurs in near shore
367 waters (Wintner and Kerwath, 2018) This could be linked to water temperature, where shallower
368 waters are warmer and therefore used during the winter. In South Africa, female *C. taurus*, which
369 have a similar long gestation period to dusky sharks, move into warmer shallower waters during
370 gestation then move south to give birth (Dicken et al., 2007). In addition, there is evidence of slight
371 seasonal variation in depth use by juvenile sandbars on the Atlantic coast of North America, where
372 dive depth increases during summer (Speed et al., 2010). Seasonal variation in depth could also be
373 linked to optimal body temperature for metabolic performance, as observed in juvenile lemon sharks
374 (Speed et al., 2010).

375 **Residency & Migration**

376 Residency index varied greatly with season and between species, but was similar between time of
377 day and sex. Highest residency was observed in sandbars, especially during the summer whereas
378 dusky sharks showed lowest residency in summer. This could reconfirm the idea that sandbars do
379 not leave Ningaloo for long periods of time as occurs in dusky sharks. RI also varied highly between
380 individuals within dusky sharks which could indicate partial migration, also observed in Port Jackson
381 and bull sharks in eastern Australia (Bass et al., 2017, Espinoza et al., 2016), and tiger sharks in
382 Hawaii (Papastamatiou et al., 2013).

383

384 Conversely, sandbars were found in the south of WA between 1994 and 1999, either indicating a
385 shift in distribution or a preference for deeper waters (Mcauley and Simpfendorfer, 2003) outside the
386 range of the acoustic receivers.

387

388 All data collected by acoustic receivers should be interpreted with caution as it only gives presence
389 or absence data but can a valuable source of relatively inexpensive long term data (Speed et al.,
390 2010, Bass et al., 2017). the close proximity of receivers within the each line array in this system
391 could have increased probability of detection however receivers in the same line were at different
392 depths, removing a proportion of this bias, however outputs should still be interpreted with reference
393 to other metrics

394 **Conclusions**

395 As species that are slow to mature and have a low fecundity (Cortés, 2000), dusky and sandbar
396 sharks are both slow to recover from overexploitation (Rogers et al., 2013). This means
397 understanding their movements is especially important. High seasonal variation and individual
398 behavioural plasticity makes predictions of movements in these species very complex. In order to
399 gain an accurate representation of broad and residential movements of both species, and to make
400 predictions, more acoustic receivers at a greater range of depths and a more standard grid network
401 would be helpful.

402 *Acknowledgements*

403

404 Thanks to the Zoological Society of London for hosting my masters project and to my primary
405 supervisor Dr David Jacoby and to the Department of Fisheries, Government of Western Australia for
406 all their help whilst working in Perth, especially my co-supervisor Dr Matias Braccini. Finally, thanks
407 to my Imperial College supervisor Dr Samraat Pawar for his patience and help with logistics.

408 *Data & Code Availability*

409

410 All R code and raw data files are available in my GitHub repository as well as a bash script detailing
411 the order to run each script file: <https://github.com/KBicks/CMEECourseWork/tree/master/Project>.

412 References

- 413 Australian Bureau of Statistics. Statistical Area Level 1 (SA1) ASGS
414 Ed 2011 Digital Boundaries in ESRI Shapefile Format., 2011. URL
415 [https://www.abs.gov.au/AUSSTATS/abs@.nsf/DetailsPage/1270.0.55.001July 2011](https://www.abs.gov.au/AUSSTATS/abs@.nsf/DetailsPage/1270.0.55.001July%202011).
- 416 R. C. Babcock, R. D. Pillans, and W. A. Rochester. Environmental and individual effects on the
417 behaviour and spawning movements of *Lethrinus nebulosus* on a coral reef. *Marine and Freshwater*
418 *Research*, 68(8):1422–1437, 2017.
- 419 Joffrey Baeyaert, David Abecasis, Pedro Afonso, Gonalo Graa, Karim Erzini, and
420 Jorge Fontes. Solo datasets’: unexpected behavioural patterns uncovered by acoustic
421 monitoring of single individuals. *Marine and Freshwater Behaviour and Physiology*,
422 51(3):1–19, 2018. ISSN 10290362. doi: 10.1080/10236244.2018.1517018. URL
423 <https://www.tandfonline.com/doi/full/10.1080/10236244.2018.1517018>.
- 424 Kamil Barton. MuMIn: Multi-Model Inference, 2019. URL
425 <https://cran.r-project.org/package=MuMIn>.
- 426 Nathan Charles Bass, Johann Mourier, Nathan A. Knott, Joanna Day, Tristan Guttridge, and Culum
427 Brown. Long-term migration patterns and bisexual philopatry in a benthic shark species. *Marine*
428 *and Freshwater Research*, 68(8):1414–1421, 2017. ISSN 13231650. doi: 10.1071/MF16122.
- 429 Douglas Bates, Martin Maechler, Benjamin M. Bolker, and Steve Walker. Fitting linear mixed-effect
430 models using lme4. *Journal of Statistical Software*, 67(1):1–48, 2015. doi: 10.18637/jss.v067.i01.
- 431 Martin T. Benavides, Rebekah L. Horn, Kevin A. Feldheim, Mahmood S. Shivji, Shelley C. Clarke,
432 Sabine Wintner, Lisa Natanson, Matias Braccini, Jessica J. Boomer, Simon J.B. Gulak, and
433 Demian D. Chapman. Global phylogeography of the dusky shark *Carcharhinus obscurus*:
434 Implications for fisheries management and monitoring the shark fin trade. *Endangered Species*
435 *Research*, 14(1):13–22, 2011. ISSN 18635407. doi: 10.3354/esr00337.
- 436 Roger Bivand, Edzer J. Pebesma, and Virgilio Gomez-Rubio. *Applied spatial data analysis with R*.
437 Springer, New York, second edition, 2013.
- 438 Roger Bivand, Tim Keitt, and Barry Rowlingson. rgdal: Bindings for the ‘Geospatial’ Data Abstraction
439 Library, 2019. URL <https://cran.r-project.org/package=rgdal>.
- 440 Benjamin M. Bolker, Mollie E. Brooks, Connie J. Clark, Shane W. Geange, John R. Poulsen,
441 M. Henry H. Stevens, and Jada Simone S. White. Generalized linear mixed models: a practical
442 guide for ecology and evolution. *Trends in Ecology and Evolution*, 24(3):127–135, 2009. ISSN
443 01695347. doi: 10.1016/j.tree.2008.10.008.

444 M. Braccini, R. McAuley, and A. Harry. Spatial and temporal dynamics of Western Australia's
 445 commercially important sharks. Technical report, Fisheries Research Division, North Beach,
 446 Western Australia, 2017a.

447 Matias Braccini. Temporal patterns in the size of the main commercial shark species of Western
 448 Australia. *Marine and Freshwater Research*, 68(6):1112–1117, 2017. ISSN 13231650. doi:
 449 10.1071/MF16117.

450 Matias Braccini and Stephen Taylor. The spatial segregation patterns of sharks
 451 from Western Australia. *Royal Society Open Science*, 3:1–7, 2016. URL
 452 <http://dx.doi.org/10.1098/rsos.160306>.

453 Matias Braccini, Alexandre Aires-da Silva, and Ian Taylor. Incorporating movement in the modelling
 454 of shark and ray population dynamics: approaches and management implications. *Reviews in Fish*
 455 *Biology and Fisheries*, 26(1):13–24, 2016. ISSN 15735184. doi: 10.1007/s11160-015-9406-x.

456 Matias Braccini, Simon de Lestang, and Rory McAuley. Dusky sharks (*Carcharhinus obscurus*)
 457 undertake large-scale migrations between tropical and temperate ecosystems. *Canadian Journal*
 458 *of Fisheries and Aquatic Sciences*, 75(9):1525–1533, 2017b. ISSN 0706-652X. doi: 10.1139/cjfas-
 459 2017-0313. URL <http://www.nrcresearchpress.com/doi/10.1139/cjfas-2017-0313>.

460 Matias Braccini, Kelly Rensing, Tim Langlois, and Rory McAuley. Acoustic monitoring reveals the
 461 broad-scale movements of commercially important sharks. *Marine Ecology Progress Series*, 577:
 462 121–129, 2017c. ISSN 01718630. doi: 10.3354/meps12251.

463 C. Calenge. The package adehabitat for the R software: tool for the analysis of space and habitat
 464 use by animals. *Ecological Modelling*, 197:1035, 2006.

465 Hamish A. Campbell, Matt E. Watts, Ross G. Dwyer, and Craig E. Franklin. V-Track: software
 466 for analysing and visualising animal movement from acoustic telemetry detections. *Marine and*
 467 *Freshwater Research*, 63:1635, 2012.

468 Shelley C. Clarke, Murdoch K. McAllister, E. J. Milner-Gulland, G. P. Kirkwood, Catherine G. J.
 469 Michielsens, David J. Agnew, Hideki Nakano, Ellen K. Pikitch, and Mahmood S. Shivji. Global
 470 estimates of shark catches using trade records from commercial markets. *Ecology Letters*, 9(10):
 471 1115–1126, 2006. doi: 10.1111/j.1461-0248.2006.00968.x.

472 Shelley C. Clarke, Shelton J. Harley, Simon D. Hoyle, and Joel S. Rice. Population Trends in Pacific
 473 Oceanic Sharks and the Utility of Regulations on Shark Finning. *Conservation Biology*, 27(1):
 474 197–209, 2013. ISSN 08888892. doi: 10.1111/j.1523-1739.2012.01943.x.

475 Enric Cortés. Life History Patterns and Correlations in Sharks. *Reviews in Fisheries Science*, 8(4):
 476 299–344, 2000. ISSN 10641262. doi: 10.1080/10408340308951115.

477 Gabor Csardi and Tamas Nepusz. The igraph software package for complex network research.
 478 *InterJournal*, Complex Sy:1695, 2006. URL <http://igraph.org>.

479 M. L. Dicken, A. J. Booth, M. J. Smale, and G. Cliff. Spatial and seasonal distribution patterns of
 480 juvenile and adult raggedtooth sharks (*Carcharias taurus*) tagged off the east coast of South Africa.
 481 *Marine and Freshwater Research*, 58(1):127–134, 2007. ISSN 13231650. doi: 10.1071/MF06018.

482 Mario Espinoza, Elodie J.I. Ledee, Colin A. Simpfendorfer, Andrew J. Tobin, and Michelle R. Heupel.
 483 Contrasting movements and connectivity of reef-associated sharks using acoustic telemetry:
 484 Implications for management. *Ecological Applications*, 25(8):2101–2118, 2015. ISSN 19395582.
 485 doi: 10.1890/14-2293.1.

486 Mario Espinoza, Michelle R. Heupel, Andrew J. Tobin, and Colin A. Simpfendorfer. Evidence of Partial
 487 Migration in a Large Coastal Predator: Opportunistic Foraging and Reproduction as Key Drivers?
 488 *PLoS ONE*, 11(2):1–22, 2016. ISSN 19326203. doi: 10.1371/journal.pone.0147608.

489 Flanders Marine Institute. World Marine Heritage Site (version 1), 2013. URL
 490 <http://www.marineregions.org/>.

491 John Fox and Sanford Weisberg. *An R Companion to Applied*
 492 *Regression*. Sage, Thousand Oaks, California, third edition, 2019. URL
 493 <https://socialsciences.mcmaster.ca/jfox/Books/Companion/>.

494 GEBCO Compilation Group. GEBCO 2019 Grid, 2019.

495 Geoscience Australia. Sunrise, Sunset & Twilight Times, 2015. URL
 496 <http://www.ga.gov.au/geodesy/astro/sunrise.jsp>.

497 Garrett Golemund and Hadley Wickham. Dates and Time Made Easy with lubridate. *Journal of*
 498 *Statistical Software*, 40(3):1–25, 2011. URL <http://www.jstatsoft.org/v40/i03/>.

499 Nigel E. Hussey, Ian D. McCarthy, Sheldon F. J. Dudley, and Bruce Q. Mann. Nursery grounds,
 500 movement patterns and growth rates of dusky sharks, *Carcharhinus obscurus*: a long-term tag
 501 and release study in South African waters. *Marine and Freshwater Research*, 60(6):571, 2009.
 502 ISSN 1323-1650. doi: 10.1071/mf08280.

503 David M.P. Jacoby and Robin Freeman. Emerging Network-Based Tools in Movement
 504 Ecology. *Trends in Ecology and Evolution*, 31(4):301–314, 2016. ISSN 01695347. doi:
 505 10.1016/j.tree.2016.01.011. URL <http://dx.doi.org/10.1016/j.tree.2016.01.011>.

506 Claudia Junge, Stephen C Donnellan, Charlie Huvaneers, Corey J A Bradshaw, Alexis Simon,
 507 Michael Drew, Clinton Duffy, Grant Johnson, Jeremy Cliff, Matias Braccini, Scott C Cutmore, Paul
 508 Butcher, Rory McAuley, Vic Peddemors, Paul Rogers, and Bronwyn M Gillanders. Comparative
 509 population genomics confirms little population structure in two commercially targeted carcharhinid
 510 sharks. *Marine Biology*, 166:16, 2019. ISSN 0025-3162. doi: 10.1007/s00227-018-3454-4. URL
 511 <https://doi.org/10.1007/s00227-018-3454-4>.

512 Jared E Knowles and Carl Frederick. merTools: Tools for analyzing mixed effect regression models,
 513 2019. URL <https://cran.r-project.org/package=merTools>.

514 James S.E. Lea, Nicolas E. Humphries, Rainer G. von Brandis, Christopher R. Clarke, and David W.
 515 Sims. Acoustic telemetry and network analysis reveal the space use of multiple reef predators and
 516 enhance marine protected area design. *Proceedings of the Royal Society B: Biological Sciences*,
 517 283(1834), 2016. ISSN 14712954. doi: 10.1098/rspb.2016.0717.

518 R Mcauley and C Simpfendorfer. Demersal Longline Fisheries , 1994 To 1999. *Fisheries Research*
 519 *Report*, 146(146):78, 2003.

520 R Mcauley, R Lenanton, J Chidlow, R Allison, and E Heist. Biology and stock assessment of the
 521 thickskin (sandbar) shark, *Carcharhinus plumbeus*, in Western Australia and further refinement of
 522 the dusky shark, *Carcharhinus obscurus*, stock assessment. Technical report, Fisheries Research
 523 Division, Western Australia, 2005. URL <http://www.fish.wa.gov.au>.

524 Rory McAuley, Barry Bruce, Ian Keay, Silas Mountford, and Tania Pinnell. *Evaluation of passive*
 525 *acoustic telemetry approaches for monitoring and mitigating shark hazards off the coast of Western*
 526 *Australia*. Number 273. 2016. ISBN 9781877098246.

527 Johann Mourier, Elodie Ledee, Tristan Guttridge, and David M P Jacoby. Network Analysis and
 528 Theory in Shark Ecology Methods and Applications. In Jeffery C Carrier, Michael R Heithaus, and
 529 Colin A Simpfendorfer, editors, *Shark Research - Emerging Technologies and Applications for the*
 530 *Field and Laboratory*, chapter 18, pages 337–356. CRC Press, Boca Raton, 1 edition, 2018.

531 J.A. Musick, R.D. Grubbs, J. Baum, and E. Cortés. *Carcharhinus obscurus*. The
 532 IUCN Red List of Threatened Species 2009: e.T3852A10127245, 2009a. URL
 533 <http://dx.doi.org/10.2305/IUCN.UK.2009-2.RLTS.T3852A10127245.en>.

534 J.A. Musick, J.D. Stevens, J.K. Baum, M. Bradai, S. Clò, I. Fergusson, R.D.
 535 Grubbs, A. Soldo, M. Vacchi, and C.M. Vooren. *Carcharhinus plumbeus*. The
 536 IUCN Red List of Threatened Species 2009: e.T3853A10130397., 2009b. URL
 537 <http://dx.doi.org/10.2305/IUCN.UK.2009-2.RLTS.T3853A10130397.en>.

538 Shinichi Nakagawa and Holger Schielzeth. A general and simple method for obtaining R^2 from
539 generalized linear mixed-effects models. *Methods in Ecology and Evolution*, 4(2):133–142, 2013.
540 ISSN 2041210X. doi: 10.1111/j.2041-210x.2012.00261.x.

541 Andrew D Olds, Rod M Connolly, Kylie A Pitt, and Paul S Maxwell. Habitat connectivity
542 improves reserve performance. *Conservation Letters*, 5:56–63, 2012. doi: 10.1111/j.1755-
543 263X.2011.00204.x.

544 Yannis P. Papastamatiou, Carl G. Meyer, Felipe Carvalho, Jonathon J. Dale, Melanie R. Hutchinson,
545 and Kim N. Holland. Telemetry and random-walk models reveal complex patterns of partial
546 migration in a large marine predator. *Ecology*, 94(11):2595–2606, 2013. ISSN 0012-9658. doi:
547 10.1890/12-2014.1. URL <http://doi.wiley.com/10.1890/12-2014.1>.

548 Edzer J. Pebesma and Roger Bivand. Classes and methods for spatial data in R. *R News*, 5(2):9–13,
549 2005. URL <https://cran.r-project.org/doc/Rnews/>.

550 David Posada and Thomas R. Buckley. Model selection and model averaging in phylogenetics:
551 Advantages of akaike information criterion and bayesian approaches over likelihood ratio tests.
552 *Systematic Biology*, 53(5):793–808, 2004. ISSN 10635157. doi: 10.1080/10635150490522304.

553 QGIS Development Team. QGIS Geographical Information System, 2019. URL
554 <http://qgis.osgeo.org/>.

555 R Core Team. R: A Language and Environment for Statistical Computing, 2015. URL
556 <https://www.r-project.org/>.

557 Paul J. Rogers, Charlie Huvaneers, Simon D. Goldsworthy, James G. Mitchell, and Laurent Seuront.
558 Broad-scale movements and pelagic habitat of the dusky shark *Carcharhinus obscurus* off
559 Southern Australia determined using pop-up satellite archival tags. *Fisheries Oceanography*, 22
560 (2):102–112, 2013. ISSN 10546006. doi: 10.1111/fog.12009.

561 Colin A Simpfendorfer, Michelle R Heupel, and Robert E Hueter. Estimation of short-term centers of
562 activity from an array of omnidirectional hydrophones and its use in studying animal movements.
563 *Canadian Journal of Fisheries and Aquatic Sciences*, 59(1):23–32, 2002. ISSN 0706-652X. doi:
564 10.1139/f01-191. URL <http://www.nrcresearchpress.com/doi/10.1139/f01-191>.

565 Conrad W. Speed, Iain C. Field, Mark G. Meekan, and Corey J.A. Bradshaw. Complexities of coastal
566 shark movements and their implications for management. *Marine Ecology Progress Series*, 408:
567 275–293, 2010. ISSN 01718630. doi: 10.3354/meps08581.

568 W. N. Venables and B. D. Ripley. *Modern Applied Statistics with S*. Springer, New York, fourth edition,
569 2002. ISBN 0-387-95457-0. URL <http://www.stats.ox.ac.uk/pub/MASS4>.

570 D. B. West. *Introduction to graph theory*. Prentice Hall, London, 2001.

571 T. Whiteway. Australian Bathymetry and Topography Grid, June 2009. Technical report, Geoscience
572 Australia, Canberra, 2009.

573 Hadley Wickham. tidyverse: Easily Install and Load the 'Tidyverse'. 2017. URL
574 <https://cran.r-project.org/package=tidyverse>.

575 Sabine P. Wintner and Sven E. Kerwath. Cold fins, murky waters and the moon: what affects shark
576 catches in the bather-protection program of KwaZulu-Natal, South Africa? *Marine and Freshwater*
577 *Research*, 69(1):167–177, 2018. ISSN 13231650. doi: 10.1071/MF17126.

578 Boris Worm, Brendal Davis, Lisa Kettemer, Christine A Ward-Paige, Demian D. Chapman,
579 Michael R. Heithaus, Steven T Kessel, and Samuel H. Gruber. Global catches, exploitation
580 rates and rebuilding options for sharks. *Marine Policy*, 40:194–204, 2013. doi:
581 10.1016/j.marpol.2012.12.034.

Table A1: GLMM outputs for network density models, using a log normal distribution. All models used individual ID as a random effect and fixed effects are given in the first column. The null model is given by network density ~ 1 , and was used as a comparison to calculate χ^2 and p-values for other models. Rows are divided into sections for both species (all, n = 111), dusky sharks (*C. obscurus*, n = 52) & sandbar sharks (*C. plumbeus*, n = 58). Metrics of fit used are Akaike Information Criterion (AIC), R^2 marginal giving the variance explained by fixed effects, and R^2 conditional giving the variance explained by the whole model, the output of the likelihood ratio test, χ^2 and p-value, and the degrees of freedom (df). Bold text indicates the best fitting model and significant metrics. Models with multiple fixed variable were also tested however single variable models had better fit.

	AIC	R_m^2	R_c^2	χ^2	df	p
<i>All</i>						
Network Density ~ 1	66.01	-	0.748	-	3	-
Network Density \sim Species	65.60	0.047	0.752	2.514	4	0.113
Network Density \sim Sex	67.52	0.049	0.755	2.692	4	0.101
Network Density \sim Season	65.09	0.032	0.763	12.47	6	0.006
Network Density \sim Time of Day	67.05	0.010	0.908	7.862	4	0.005
<i>Carcharhinus obscurus</i>						
Network Density ~ 1	59.45	-	0.779	-	2	-
Network Density \sim Sex	59.95	0.130	0.785	3.436	4	0.064
Network Density \sim Season	48.39	0.159	0.850	20.28	6	<0.001
Network Density \sim Time of Day	58.66	0.021	0.933	10.26	4	0.0013
Network Density \sim Migratory Status	60.47	0.034	0.778	0.738	4	0.390
<i>Carcharhinus plumbeus</i>						
Network Density ~ 1	7.460	-	0.709	-	3	-
Network Density \sim Sex	9.420	0.012	0.712	0.334	4	0.563
Network Density \sim Season	5.115	0.033	0.733	8.172	6	0.042
Network Density \sim Time of Day	8.456	0.005	0.870	1.295	4	0.255

Table A2: GLMM outputs for kernel density utilisation models (KUD), using a gamma distribution. All models used individual ID as a random effect and fixed effects are given in the first column. The null model is given by $KUD \sim 1$, and was used as a comparison to calculate χ^2 and p-values for other models. Rows are divided into sections for both species (all, $n = 77$), dusky sharks (*C. obscurus*, $n = 39$) & sandbar sharks (*C. plumbeus*, $n = 39$). Metrics of fit used are Akaike Information Criterion (AIC), the output of the likelihood ratio test, χ^2 and p-value, and the degrees of freedom (df). Two types of AIC are used as sample size was too small to subset both season and time of day, giving two subsets with non comparable AIC values (se = seasonal subset and dn = time of day subset). Bold text indicates the best fitting model and significant metrics. Models with multiple fixed variable were also tested however single variable models had better fit.

	AIC_{se}	AIC_{dn}	χ^2	df	p
<i>All</i>					
KUD ~1	345.0	288.3	-	3	-
KUD ~Species	334.9	285.8	12.13	4	<0.001
KUD ~Sex	346.5	289.8	0.584	4	0.445
KUD ~Season	347.3	-	3.702	6	0.230
KUD ~Time of Day	-	289.8	0.476	4	0.491
<i>Carcharhinus obscurus</i>					
KUD ~1	178.2	163.1	-	3	-
KUD ~Sex	178.2	162.2	2.032	4	0.154
KUD ~Season	181.8	-	2.485	6	0.478
KUD ~Time of Day	-	165.1	0.089	4	0.765
KUD ~Migratory Status	179.5	164.1	0.703	4	0.402
<i>Carcharhinus plumbeus</i>					
KUD ~1	153.4	124.1	-	3	-
KUD ~Sex	155.4	126.1	0.007	4	0.935
KUD ~Season	158.3	-	1.020	6	0.796
KUD ~Time of Day	-	123.6	2.52	4	0.112

Table A3: GLMM outputs for residency index models (RI), using a log normal distribution. All models used individual ID as a random effect and fixed effects are given in the first column. The null model is given by $RI \sim 1$, and was used as a comparison to calculate χ^2 and p-values for other models. Rows are divided into sections for both species (all, $n = 110$), dusky sharks (*C. obscurus*, $n = 49$) & sandbar sharks (*C. plumbeus*, $n = 59$). Metrics of fit used are Akaike Information Criterion (AIC), R^2 marginal giving the variance explained by fixed effects, and R^2 conditional giving the variance explained by the whole model, the output of the likelihood ratio test, χ^2 and p-value, and the degrees of freedom (df). Two types of AIC are used as sample size was too small to subset both season and time of day, giving two subsets with non comparable AIC values (se = seasonal subset and dn = time of day subset). Bold text indicates the best fitting model and significant metrics. Models with multiple fixed variable were also tested however single variable models had better fit.

	AIC_{se}	AIC_{dn}	R_m^2	R_c^2	χ^2	df	p
<i>All</i>							
RI ~ 1	-646.3	-1076.0	-	0.992	-	3	-
RI ~ Species	-345.8	-1075.7	0.038	0.992	1.422	4	0.233
RI ~ Sex	-644.9	-1074.4	0.018	0.992	0.605	4	0.437
RI ~ Season	-730.7	-	0.037	0.994	90.38	6	<0.001
RI ~ Time of Day	-	-1217.6	0.006	0.999	143.6	4	<0.001
<i>Carcharhinus obscurus</i>							
RI ~ 1	-404.8	-610.0	-	0.996	-	3	-
RI ~ Sex	-406.0	-608.3	0.182	0.996	2.155	4	0.142
RI ~ Season	-461.8	-	0.222	0.998	63.00	6	<0.001
RI ~ Time of Day	-	-740.5	0.050	0.999	132.5	4	<0.001
RI ~ Migratory Status	-403.7	-734.9	0.060	0.996	0.921	4	0.337
<i>Carcharhinus plumbeus</i>							
RI ~ 1	-299.1	-509.8	-	0.989	-	3	-
RI ~ Sex	-297.4	-507.9	0.015	0.989	0.288	4	0.592
RI ~ Season	-349.0	-	0.033	0.991	55.92	6	<0.001
RI ~ Time of Day	-	-589.1	0.004	0.999	81.29	4	<0.001

Table A4: GLMM outputs for daily detection models (RI), using a log normal distribution. All models used individual ID as a random effect and fixed effects are given in the first column. The null model is given by number of detections ~ 1 , and was used as a comparison to calculate χ^2 and p-values for other models. Rows are divided into sections for both species (all, $n = 100$), dusky sharks (*C. obscurus*, $n = 30$) & sandbar sharks (*C. plumbeus*, $n = 40$). Metrics of fit used are Akaike Information Criterion (AIC), R^2 marginal giving the variance explained by fixed effects, and R^2 conditional giving the variance explained by the whole model, the output of the likelihood ratio test, χ^2 and p-value, and the degrees of freedom (df). Two types of AIC are used as sample size was too small to subset both season and time of day, giving two subsets with non comparable AIC values (se = seasonal subset and dn = time of day subset). Bold text indicates the best fitting model and significant metrics. Models with multiple fixed variable were also tested however single variable models had better fit.

	AIC_{se}	AIC_{dn}	R_m^2	R_c^2	χ^2	df	p
<i>All</i>							
Det ~ 1	101930	124948	-	0.221	-	3	-
Det \sim Species	101932	124949	<0.001	0.220	0.180	4	0.671
Det \sim Sex	101930	124947	<0.001	0.216	2.083	4	0.149
Det \simSeason	101232	-	<0.001	0.234	260.4	7	<0.001
Det \sim Time of Day	-	124915	<0.001	0.155	34.72	4	< 0.001
Det \sim Depth Band	101477	124549	<0.001	0.233	463.4	8	< 0.001
<i>Carcharhinus obscurus</i>							
Det ~ 1	7406.3	7895.9	-	0.140	-	3	-
Det \sim Sex	7407.5	7897.1	<0.001	0.137	0.813	4	0.367
Det \sim Season	7399.0	-	<0.001	0.152	13.30	6	0.004
Det \sim Time of Day	-	7890.1	<0.001	0.120	7.861	4	0.005
Det \sim Migratory Status	7408.0	7897.4	<0.001	0.139	0.276	4	0.600
Det \simDepth Band	7354.9	7846.9	0.0012	0.136	59.35	7	< 0.001
<i>Carcharhinus plumbeus</i>							
Det ~ 1	93174	116707	-	0.231	-	3	-
Det \sim Sex	93174	116707	<0.001	0.224	1.365	4	0.243
Det \simSeason	92927	-	<0.001	0.244	252.6	6	< 0.001
Det \sim Time of Day	-	116678	<0.001	0.177	31.26	4	< 0.001
Det \simDepth Band	92733	116303	<0.001	0.235	450.8	8	< 0.001